Assessing the Contribution of Nightly Rechargeable Grid-Scale Storage to Generation Capacity Adequacy

Gruffudd Edwards[a], Sarah Sheehy[b], Chris J. Dent[a,*], Matthias C. M. Troffaes[c]

[a] *School of Mathematics, University of Edinburgh, UK*
[b] *School of Engineering & Computing Sciences, Durham University, UK*
[c] *Department of Mathematical Sciences, Durham University, UK*

Abstract

This paper is concerned with assessing the contribution of grid-scale storage to generation capacity adequacy. Results are obtained for a utility-scale exemplar involving the Great Britain power system. All stores are assumed, for the purpose of capacity adequacy assessment, to be centrally controlled by the system operator, with the objective of minimising the Expected Energy Not Served over the peak demand season. The investigation is limited to stores that are sufficiently small such that discharge on one day does not restrict their ability to support adequacy on subsequent days. We argue that for such stores, the central control assumption does not imply loss of generality for the results.

Since it may be the case that stores must take power export decisions without the benefit of complete information about the state of the system, a methodology is presented for calculating bounds on the value of such information for supporting generation adequacy. A greedy strategy is proven to be optimal for the case where decisions can be made immediately after a generation shortfall event has occurred, regardless of the decision maker's risk aversion. The adequacy contribution of multiple stores is examined, and algorithms for coordinating their responses are presented.

Keywords: Storage, Generation Adequacy, Optimal Strategies, Coordination Algorithm

1. Introduction

The flexibility offered by grid-scale electrical energy storage plays a crucial role in lowering the cost of power delivered by future low carbon networks, whilst maintaining their reliability [1, 2, 3, 4]. For example, the International Electrotechnical Commission states in [3] that storage will become indispensable in emerging energy markets. The World Energy Council in [4] describes recent

*Corresponding author
Email address: chris.dent@ed.ac.uk (Chris J. Dent)

developments in storage technology as game-changing in terms of solving the intermittency challenge of wind and solar generation.

The cost savings associated with the presence of significant storage capacity in future systems include reductions in capital expenditure on generation, transmission and distribution infrastructure along with reduced operating costs [1]. While it is argued in [4] that many analyses focus on the high costs of storage without fully evaluating potential savings, it was suggested in [2] that these savings will be of the order of $\$10^9$ to $\$10^{10}$/year for the GB system by 2030.

This paper concerns assessing the capacity adequacy contribution of grid-scale storage, i.e. the contribution of stores in ensuring that the risk of failing to meet demand is kept appropriately low at all times. Previous work in the literature has examined capacity adequacy for a range of assumed objectives for a storage operator, including adequacy support [5, 6], smoothing renewable output [5, 7], minimising system costs [8], and maximising profit [9, 10].

This paper provides a new approach to assessing the capacity adequacy contribution of storage, based on a number of reasonable assumptions which both simplify computation and add transparency in interpretation of results: (a) in a system with a relatively small storage capacity (in the sense described in Section 4.1) the storage will be able to recharge fully overnight, and (b) within the adequacy risk assessment storage is modelled as acting entirely to reduce adequacy risk (which as discussed in Section 4.1 does not imply that storage will act in this way in normal operation – storage's contribution to mitigating adequacy risk is about what it can do if needed, not what it will do when the system is not under stress). Even if storage is not directly controlled by the System Operator, it is reasonable to think that it will act to mitgate risk, either through prices being high at times of system stress, or the System Operator coordinating discharge of stores in the real time market. Making these assumptions greatly simplifies the analysis, and improves transparency of the model and drivers of results.

Storage's contribution is assessed assuming that the goal is to minimise Energy Not Served (ENS), implying a headline risk index of Expected Energy Not Served (EENS) – using Loss of Load Expectation (LOLE) as the headline index, as is more common, would imply a strong preference for short deep shortfalls over longer shallow ones which is likely to not be the preference of actual system operators.

This paper investigates the relationship between a store's energy and power export capacities and the consequent reduction in EENS that can be delivered. All works cite above assume that operators can and will respond to generation shortfall events in real time as they occur. Further, these works take as given that stores able to respond in this should adopt a 'greedy' strategy, i.e. they export sufficient energy as possible to mitigate any shortfall, without holding back for future periods – a rigorous proof of the optimality of this strategy is presented here for the case of a single store.

The cases where storage can be scheduled in real time, and where it must be scheduled so far ahead of real time that only a generic storage schedule which can be repeated each day, are compared – this allows assessment of the benefits

of real time information. In addition, the case of a single store is compared with multiple stores having the same total power and energy capacities, under a range of possible algorithms for coordinating multiple stores – To the best of our knowledge, this paper is the first to consider the multiple store case in this way.

The results obtained are for a utility-scale exemplar based on the Great Britain (GB) power system. The primary contributions of this paper are however methodological, and applicable to any system for which the modelling assumptions are relevant. The paper proceeds with a literature review in section 2, presentation of our general system model in section 3, and presentation of the problem to be solved in section 4, including storage power exports as decision functions. Section 5 outlines details of the chosen exemplar, while section 6 presents results. Section 7 concludes the paper.

2. Previous Work on Adequacy and Storage

When assessing the adequacy contribution of storage there are several basic questions that must be addressed at the outset, including the objective of the storage operator(s) and the extent to which stores may be coordinated by the system operator, and the information available at the time decisions on scheduling of storage must be made. This section reviews the limited existing literature on the contribution of storage to adequacy, with reference to the way these questions are addressed. Further citations may be found in the PhD thesis of Gafurov [11], which presents a taxonomy of assumed objectives of the storage operator.

The simplest approaches are those where the assumed objective does not explicitly involve economics. Within this broad category, the simplest are those assuming that the storage operator seeks to make the strongest possible contribution to adequacy, by attempting to mitigate shortfall events whenever they occur. As discussed in the previous section, this operator objective – combined with the ability to respond in real time – is assumed in several works, including Zheng *et al.* [6]. It is also one of several objectives explored by Hu *et al.* [5] which similarly assumes that storage export decisions are taken in real time. The present paper extends the methodology presented in such examples by exploring the impact of making decisions ahead of real time, i.e. with incomplete information about the timing and magnitude of shortfalls.

An alternative operator objective assumed by some authors is smoothing the joint production from variable renewable energy generators and storage. Variants of this objective are by explored by Hu *et al.* in [5], also Wang and Bai in [7]. The motivation for this operator objective is not precisely specified, but might reflect a situation where the storage is operated by a generation company trading energy from variable generators in a futures market, seeking to minimise penalties associated with generation forecast errors. It should be noted that this objective is not directly aimed at mitigating adequacy risk.

Other previous authors have introduced economic considerations directly into their capacity adequacy assessment methodology. This can be in the form

of stores controlled by the system operator, seeking to minimise system costs, or independent stores operated to maximise profit. Tuohy and O'Malley in [8] are an example of the former, and consider a single pumped hydro storage scheme within an economic dispatch for the power system. They assume that decisions taken ahead of real time are over-ridden in the event of a generation shortfall, with the store exporting as much as possible to mitigate the shortfall. However the dispatch does not explicitly consider the possibility of future shortfalls, and no full risk calculation is performed (instead a capacity value is specified based on the energy in store during the most risky subset of time periods). Broadly the same approach to assessing capacity value is adopted by Madaeni *et al.* in [12], who consider a thermal storage unit integrated with a concentrating solar power plant – however the operator's objective in this case is to maximise profit.

Sioshansi *et al.* [9] develop this approach further, with the assumed objective of maximising profit. Dynamic programming is used to schedule storage ahead of real time for price arbitrage, but these decisions are changed in the event of a shortfall. Unlike [8, 12], this work performs a risk based capacity value calculation. However, within this risk calculation the storage unit is represented as an equivalent conventional unit based on the results of the economic optimisation, which (again within the risk calculation) does not acknowledge the finite energy capacity of the storage unit. While this finite energy capacity may (to an extent) be represented indirectly in the way the inputs to the risk calculation are specified, the complexity of the two (economic and risk) stage calculation process makes linking the explicit and implicit assumptions in the study to a given real world situation challenging.

Cruise and Zachary in [10] also consider storage operated with the objective of profit maximisation. They allow revenue to come both from arbitrage and by offering 'buffering services', i.e. a willingness to export in the event of a shortfall. Thus, in their model storage dispatch is both planned in advance and may be adjusted in real time, and in this case the planned dispatch maximises the expected profit from both sources. While their work does not investigate the adequacy contribution of storage, the optimal charging-discharging schedules they derive could in principle serve as a basis for such calculations, since the value of real-time decision-making is accounted for.

3. System Model

3.1. EENS Calculations Without Storage

This section outlines the model for the power system without storage, and explains how the expected energy not served is calculated. Without loss of generality we work in hourly time steps, to reflect the data available and to simplify notation. All results apply equally to other time steps. Notation is as follows: t is the hour within the peak demand season (between 0 and T), and D_t, X_t and Y_t are respectively the demand, available conventional capacity and available renewable capacity (all in MW) at time t. Capital letters indicate random variables (with the exception of T), while realised values are represented by the same letters in lower case.

We are interested in the balance of demand and available generation capacity for each time step (rather than generation dispatch) i.e. $D_t - X_t - Y_t$. This balance is usually negative, but there is always some probability that it is positive, which represents a generation shortfall event. The energy not served over a period of length T is then given by:

$$\text{ENS} := \sum_{t=0}^{T} \max\{0, D_t - X_t - Y_t\}, \tag{1}$$

while its expected value is:

$$\text{EENS} = \mathbb{E}(\text{ENS}) = \mathbb{E}\left(\sum_{t=0}^{T} \max\{0, D_t - X_t - Y_t\}\right) \tag{2}$$

$$= \sum_{t=0}^{T} \mathbb{E}(\max\{0, D_t - X_t - Y_t\}). \tag{3}$$

To evaluate this expression, it is necessary to obtain not only the marginal probability distributions of D_t, X_t, and Y_t, but also their joint distribution at time t. Although the distribution of ENS will obviously depend also on the time correlations between the variables, for this case without storage, the EENS does not depend on time correlations due to the standard result that the expected value of a sum of random variables is equal to the sum of their expected values.

There is an active debate regarding whether adequacy assessments in systems with high renewable penetrations should also consider detail of system operation, such as the ability to manage rapid changes in net demand, and uncertainty in short term forecasts [13]. The methodology described in the present paper is applicable to the adequacy problem as traditionally specified, and thus evaluates only the component of the reliability index arising from capacity shortfalls at times of highest demand – we do note however that in some systems it will be possible to perform adequacy and flexibility risk assessments separately, if there is a very small chance of both being an issue at the same time, even though in principle they should be considered together in system planning. Where these issues of system operation are relevant, higher time resolution data and modelling may be required.

Network constraints are not considered here, as is common practice in practical adequacy studies. In Great Britain the transmission network is heavily built, and active network constraints biting are likely to signify high output from remote wind generation rather than any additional adequacy risk [14]. However this simplification might be less realistic in other systems when relating calculated adequacy risk to real world risk to end user supply, despite it being widespread practice.

The random processes for D_t, X_t and Y_t are all assumed to be statistically independent of each other for the purpose of the exemplars in this paper. In reality, one would expect some statistical dependence between renewable generation and demand due to influence of weather on each of them. In the absence

of a readily available joint time series model for wind and demand in any system (including GB), this provides a sufficiently representative model of GB conditions to demonstrate the new proposed approach to modelling of storage.

Time series models are used for the conventional and renewable capacity availability processes. However, due to the highly complex nature of demand, we adopt a *hindcasting* approach, whereby the joint distributions are conditioned on historical demand traces. Assuming that both conventional and renewable generation are independent of demand, Eq. (3) becomes:

$$\mathrm{EENS} = \mathbb{E}(\mathrm{ENS}|D_0 = d_0, \ldots, D_T = d_T) \tag{4}$$

$$= \sum_{t=0}^{T} \mathbb{E}(\max\{0, d_t - X_t - Y_t\}). \tag{5}$$

3.2. Introduction of Storage

In this subsection the system model is extended to include a single energy store. The store is assumed to have constant power output capacity $\overline{s}$ and usable energy storage capacity $\overline{e}$. Occasionally, we will also refer to $\overline{h} := \overline{e}/\overline{s}$, representing the length of time for which an initially full store can export at maximum capacity before it is empty.

The storage output at time t is labelled s_t, with positive values indicating that energy is being exported. The usable energy remaining in the store at the beginning of hour t is

$$e_t := \overline{e} - \sum_{\tau=0}^{t-1} s_\tau \tag{6}$$

so we assume that the store does not leak energy. The dependence of e_t on past exports obviously introduces a temporal coupling to the system model. We also define $h_t := e_t/\overline{s}$, i.e. the length of time for which the store at time t can export at maximum capacity before it is empty. The present formulation excludes pumped storage schemes where there is significant flow into the upper reservoir; including this effect would be a simple extension to the 'real time decisions' formulation in Section 4.3. In addition (as is currently the case in GB and possibly other systems) pumped storage plants may have a sufficiently high energy to power ratio that finite energy capacity does not restrict their contribution to capacity adequacy [14].

The formulation also excludes the possibility of storage recharging within day (for the GB exemplar used, no example where this would have been relevant was found in 100,000 Monte Carlo realisations of the season under study.) The reason for this is seen in Fig. 1, where there is a single distinct daily demand peak, and thus the shortfalls seen in the exemplar are all continuous periods of high demand low wind output. It would be a simple matter to add within-day recharging during periods where there is no shortfall if this was important in a different exemplar (for instance in a summer peaking system with a high solar penetration, where the daily trace of demand-net-of-solar-output might contain

two clear peaks). A further straightforward addition would be to include in the probability model the possibility of storage being mechanically unavailable.

The storage export at time t is a decision variable, and a function of the information about the state of the system at time t. We denote that information here by the vector R_t. This vector might include the availability of each generator during recent time periods, recent renewable generation, prices in a balancing market, amongst other things. As an example, consider the case where storage is controlled by a system operator (SO), purely concerned with securing adequate supply. The SO is able to make storage export decisions in real time, immediately following the realisation of generation availabilities. In this case, the information vector might be

$$R_t := (\mathbf{X}_0, \mathbf{Y}_0, \ldots, \mathbf{X}_t, \mathbf{Y}_t) \tag{7}$$

where each $\mathbf{X}_k$ might represent the vector of available capacities over all conventional generators, and each $\mathbf{Y}_k$ might represent the vector of outputs over all renewable generators, for $k \in \{0, 1, \ldots, t\}$, and where $k = 0$ represents the beginning of the period for which the EENS is to be minimised. Information from times before $t = 0$ could also be considered if relevant.

Consider the case where the store is again controlled by the SO, but for some technical reason decisions must be taken ahead of real time. In this case, the information vector might be

$$R_t := (\mathbf{X}_0, \mathbf{Y}_0, \ldots, \mathbf{X}_{t-\tau}, \mathbf{Y}_{t-\tau}) \tag{8}$$

if the decision must be taken τ hours in advance.

We assume that knowledge of R_t implies knowledge of $R_0, \ldots, R_{t-1}$. In this case, storage export decisions can be written as $s_t(R_t)$. Any vector of export decisions spanning the period of interest is referred to here as a strategy, and is denoted as s. So,

$$s(R_T) = (s_0(R_0), \ldots, s_T(R_T)). \tag{9}$$

Given a strategy s, the EENS for the period of interest is given by $\mathbb{E}[\mathrm{ENS}(s)]$, where

$$\mathrm{ENS}(s) = \sum_{t=0}^{T} \max\{0, d_t - s_t(R_t) - X_t - Y_t\}. \tag{10}$$

3.3. Multiple Stores

This paper will explore the capacity adequacy contribution of multiple stores, and compare the results to a single store with the same total energy and power capacities. A set of N stores is considered, with individual energy capacities $\overline{e}_i$, power capacities $\overline{s}_i$, and discharge times from full of $\overline{h}_i$. The discharge time from full of the set is the largest $\overline{h}_i$ value. At time t, the stores have energy contents e_{it}, and collectively could fully mitigate a shortfall of magnitude

$$\overline{s}_t^{\,\mathrm{eff}} = \sum_{i=1}^{N} \min\{\overline{s}_i, e_{it}\}, \tag{11}$$

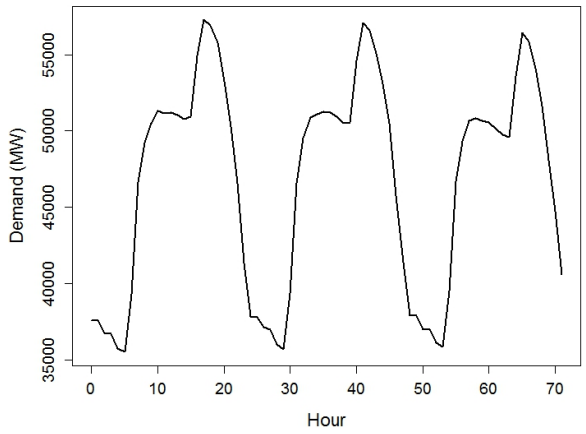

Figure 1: A 3-day sample of system demand, rescaled from the historic data for winter 2010-11.

where $\overline{s}_t^{\text{eff}}$ may be described as the effective capacity of the set at time t. Export decisions are written as $s_{it}(R_t)$.

Since

$$\overline{s}_t^{\text{eff}} \leq \min\left\{\sum_{i=1}^{N}\overline{s}_i,\ \sum_{i=1}^{N}e_{it}\right\}, \tag{12}$$

multiple stores will not always be able to reduce EENS by the same amount as a single store with the same total energy and power capacities. Clearly the extent of reduction in performance depends on the way in which the total energy and power capacities are divided among the multiple stores, along with the method of coordination for discharging the individual stores.

4. Optimal Storage Decisions

4.1. The System Operator's Problem

We consider a system operator (SO), concerned with minimising a suitable capacity adequacy metric by choosing optimal storage export strategies. A commonly adopted adequacy metric is the Loss of Load Expectation (LOLE): the expected value of the number of time-periods per year where there is a generation shortfall. However we believe that the EENS is a more suitable objective to be minimised than the LOLE, since the latter would unduly reward shifting unserved energy into fewer but deeper shortfall periods.

When a very large amount of storage is present in power systems – such as the hydro-dominated systems of Norway, Brazil and the Pacific North West of the USA – there is an economic balance to be struck in operation between using zero marginal cost energy immediately, and holding energy in reserve to support

future adequacy. It is then only meaningful to calculate a risk level conditional on a particular operational strategy, rather than there being a single risk level for the system which could be realised in practice – the risk minimising strategy would be only to discharge storage when there is insufficient other capacity to meet demand, which is clearly unrealistic when looking to store energy between days for price arbitrage.

This paper limits its scope to systems with relatively small total storage capacities, in the sense that discharge of a store on one day does not restrict its ability to support adequacy on subsequent days, due to the opportunity to recharge overnight. Moreover, on days where there is a possibility of a shortfall due to an absolute shortage of generating capacity, price differences will typically incentivise storage to charge overnight to the extent required to make its full contribution to adequacy – thus, for the purpose of adequacy calculation, such stores may be assumed full each morning.

'Small' for this purpose also implies that the storage capacity is substantially less than that required to flatten the daily demand trace, and thus can include grid scale storage with aggregate capacity measured in GWh – in order to illustrate the relevant energy and capacity scales, an example demand trace from GB is provided in Fig. 1. There may also be other considerations in defining 'small', for instance in GB there may be additional detail of system operation and storage coordination to be considered once storage capacity is sufficiently large to fill in the early evening darkness peak (which rises about 5 GW above the daytime demand plateau).

Since prices are high during times of system stress, stores operated for profit on a merchant basis will naturally tend to be available at such times. Assuming that they offer their services in the real time market, the System Operator (SO) would then be able to dispatch them, making a centrally-coordinated view of storage reasonable for assessing capacity adequacy even in a liberalised market. If the SO does not have direct control, or for instance can only incentivise stores to be available at certain times of day, then this might best be treated by building a stochastic model of storage availability across the day to reflect this lack of direct control – however this case is not the subject of the paper.

For the purpose of the adequacy risk model, it will be assumed that storage acts entirely to support adequacy. This is based on the observation that storage's contribution to adequacy is about what it can do when needed, not what it will do on the large majority of days when the system is not under stress – thus assuming within the risk model that storage acts to support adequacy does not imply that the resulting dispatch will be implemented unless the storage is required to mitigate a capacity shortfall (a similar argument about carrying no implication of how storage would operate on days where there is no system stress applies to the assumption of recharging overnight). Given the way that the risk calculations for different days then separate, in this 'small storage' regime it is then meaningful to specify a single level of risk for the system based on a risk-minimising strategy.

Beyond these economic justifications for the assumptions made, we also note that the maximum extent to which storage can mitigate adequacy risk if fully

coordinated is also of interest in itself – if these assumptions are not deemed to be entirely realistic in a given system, then clearly making them provides an upper bound on the true risk level.

4.2. Feasible Strategies

The problem faced by a SO may be expressed as

$$\min_{s\in\mathbb{S}} \mathbb{E}[\mathrm{ENS}(s)], \tag{13}$$

where ENS(s) is given by Eq. (10), and $\mathbb{S}$ is the set of *feasible* strategies. For a strategy to be feasible, it must satisfy both power and energy constraints. The former, reflecting the finite power export capacity of a store, is simply

$$0 \le s_t(R_t) \le \overline{s}. \tag{14}$$

Before formulating the energy constraint, it is useful to decompose t in terms of the day within the peak demand season, and the hour within that day, according to

$$t = 24u + v \tag{15}$$

The daily index u ranges from 0 to $U = \frac{T+1}{24} - 1$, while the hour of day v ranges from 0 to 23. Since it is assumed that stores are full at the beginning of each day, it follows that if e.g. 6am is chosen as $t = 0$, then $e_t = \overline{e}$ whenever $v = 0$. Since total energy exported from a store during a day cannot exceed its capacity, the energy constraint is:

$$\forall\ u: \quad \sum_{v=0}^{23} s_{24u+v}(R_{24u+v}) \le \overline{e}. \tag{16}$$

As a result of the assumption of nightly recharging, the efficiency of stores does not feature in the analysis. This is because storage parameters are defined in terms of exportable power and energy. Round trip efficiency then determines the energy required to refill the stores, which is irrelevant to the analysis.

For multiple stores, the optimisation problem is essentially the same, except that the strategy s relates to the output from each store, and

$$s_t(R_t) := (s_{1t}(R_t), \ldots, s_{Nt}(R_t)). \tag{17}$$

A possible further extension to the system model, as seen in [15], would be to introduce flexible demand response, which helps the system avoid shortfalls by deferring some of it's demand away from peak times. Demand response differs from storage only in that it might not be necessary to pay back all of the deferred energy demand. Since the approach adopted here does not explicitly consider the charging of stores – the equivalent of paying back deferred load – it is irrelevant whether or not this payback must be in full. There is therefore no distinction between storage and demand response. That is, a store with capacity parameters $\overline{e}$ and $\overline{s}$ is indistinguishable from demand response where the total

amount of energy that may be deferred from peak hours is $\overline{e}$, and no more than $\overline{s}$ of load can be deferred at any time. A system with multiple customer groups with different willingness to defer load may be represented as a set of multiple stores.

4.3. Real Time Decisions

Consider first the case of a single store where the SO is in the ideal position of making power export decisions immediately after the realisation of the supply–demand balance for each hour. One of the main contributions of this paper is to demonstrate that there exists a feasible strategy s^* which not only minimises the expected value of the ENS, but in fact minimises the ENS for all possible random outcomes of the system.

For a single discharge cycle, this is the greedy strategy given by:

$$s_t^*(r_t) := \min\{\max\{0, d_t - x_t - y_t\},\ \overline{s},\ e_t^*\} \tag{18}$$

where

$$e_t^* := \overline{e} - \sum_{\tau=0}^{t-1} s_\tau^*(r_\tau). \tag{19}$$

That is, the store exports as much as possible in the event of a shortfall – up to the level of the shortfall, or as much as the energy and power export constraints allow. This result is proven for a single day (i.e. one discharge cycle) in Appendix A.

From Eq. (10) and Eq. (15), we have that

$$\mathbb{E}[\mathrm{ENS}(s)] = \sum_{u=0}^{U} \mathbb{E}[\mathrm{ENS}_u(s_u)], \tag{20}$$

where ENS_u is the energy not served on day u, and s_u is the strategy for that day. We may therefore decompose the seasonal optimisation problem into the set of daily problems, i.e.

$$\min_{s\in\mathbb{S}} \sum_{u}^{U} \mathbb{E}[\mathrm{ENS}_u(s_u)] = \sum_{u}^{U} \min_{s_u\in\mathbb{S}_u} \mathbb{E}[\mathrm{ENS}_u(s_u)], \tag{21}$$

where $\mathbb{S}_u$ is the feasible strategy space for one day. Therefore, since it is established in Appendix A that the greedy strategy is optimal for each day, it follows that the greedy strategy is optimal for the entire season.

An interesting feature of this result is that the only information required to make an optimal decision at time t is the (already realised) balance of demand and generation, $d_t - x_t - y_t$. Also interesting is the implication with regard to the risk aversion of the SO. Whereas a risk-neutral decision maker is interested in minimising the expected ENS, a more risk-averse operator is more motivated by avoiding the most serious possible shortfall events. Such a decision maker seeks to minimise some high percentile of the ENS. Since the greedy strategy

minimises the ENS for every possible outcome of available supply, it follows that it is optimal regardless of the decision maker's risk aversion level. This makes Eq. (18) a more powerful result than if the greedy strategy minimised the expectation only.

4.4. Decisions Ahead of Real Time

This section considers decisions made ahead of real time, when the information available to the SO is incomplete. In such cases, the ENS remains defined by Eq. (10), but R_t may no longer imply full knowledge of X_t and Y_t. Generally, making decisions on the basis of partial information leads to multi-stage stochastic optimisation problems which can be very hard to solve.

The situation is much simpler for the special case where storage decisions are taken far in advance of real time. In this case no information is available at time t, so we can set $R_t = 0$ and we have a straightforward multi-dimensional single-stage stochastic optimisation problem. This is referred to as the 'far ahead case', and represents the worst case scenario for the decision maker, in terms of available information. It allows the analysis to bound the contribution that a store of a given power and energy capacity can make to supporting capacity adequacy.

In addition to having no information about X_t and Y_t, it is assumed that the SO does not know the demand in advance – but does know its empirical distribution for each hour of the day. As a result, the SO's objective is to find a single profile, to be repeated every day, which minimises the seasonal EENS value. Since the empirical distribution of demand is represented in the system model by a hindcast trace, the entire trace must be used to establish the optimal repeated profile. The SO's problem may then be written as the following optimisation problem:

$$\min_{s\in\mathbb{S}}\left\{\sum_{u=0}^{U}\sum_{v=0}^{23}\mathbb{E}[\max\{d_{24u+v}-s_v-X_{24u+v}-Y_{24u+v},\ 0\}]\right\}, \tag{22}$$

where through stationarity of the relevant processes the $\{X_{24u+v}\}$ are identically distributed, as are the $\{Y_{24u+v}\}$. The summand may thus be rewritten as $\mathbb{E}[\max\{d_{24u+v}-s_v-X-Y,\ 0\}]$, where X and Y are the marginals of the available conventional and renewable capacity processes respectively.

Using integration by parts, this problem can be reformulated as

$$\min_{s\in\mathbb{S}}\left\{\sum_{u=0}^{U}\sum_{v=0}^{23}g(d_{24u+v}-s_v)\right\}, \tag{23}$$

where

$$g(\zeta)=\int_{z=0}^{\zeta}F_Z(z)\mathrm{d}z, \tag{24}$$

and $Z = X + Y$. This expression allows efficient numerical solution of the optimisation, with no subsequent simulation required to evaluate the EENS.

4.5. Multiple Stores

4.5.1. Objective: Maintaining Effective Capacity

This section explores principles and methods for the coordination of multiple stores, that allow good decisions to be made when the stores are responding in real time with the objective of minimising EENS.

Consider a set of N stores responding to a generation shortfall during some time step t. For convenience, we introduce Φ_t to represent the shortfall, with realised values φ_t, i.e.

$$\Phi_t = \max\{d_t - X_t - Y_t,\ 0\}. \tag{25}$$

We already saw that the optimal greedy strategy with full information for a single store is to export as much power as possible, up to the level of the shortfall. Logically, the total output from a set of stores should also follow the greedy strategy. However, this condition is not sufficient to arrive at an optimal multi-store strategy.

The maximum shortfall that may be entirely mitigated by the set of stores, is $\overline{s}_t^{\text{eff}}$, as defined by Eq. (11) in section 3.3. A good decision at time t is one that follows the greedy strategy, and does so in such a way that retains the effective capacity of future periods as much as possible. This means taking care to preserve individual future effective capacities, $\min\{e_{i\tau}, \overline{s}_i\}$, as much as possible. To achieve this, we present and examine two heuristic strategies:

(i) Sequential-greedy approach. The stores are discharged sequentially, in some sensible order – e.g. by decreasing $\overline{h}_i$.

(ii) Proportional discharge. The stores are all discharged simultaneously and in proportion to their remaining energy content – so that each store can contribute something until they are all empty.

Algorithms to implement these strategies are presented in the following sections. As we shall see, neither strategy is optimal in all situations. However, the difference in performance is very small (moreover we have tried further algorithm variants and a wider range of text systems without finding substantial differences in performance on realistic examples) – thus we believe that for practical applications, either strategy is near optimal, and that when making real world predictions any differences in performance will be dominated by other aspects of modelling uncertainty.

4.5.2. Sequential-Greedy Coordination

For the sequential-greedy approach, in the event of a shortfall at hour t the procedure is:

1. Assign a discharge order for the stores.

2. Discharges store 1 according to the greedy strategy, so that

$$s_{1t}^* = \min\{\phi_t,\ e_{1t},\ \overline{s}_1\}. \tag{26}$$

3. If $\phi_t > s^*_{1t}$, i.e. the first store was not able to fully mitigate the shortfall, then the 2nd store in the order must export in a greedy manner, such that

$$s^*_{2t} = \min\{\phi_t - s^*_{1t},\ e_{2t},\ \overline{s}_2\}. \tag{27}$$

4. Progress through the ordered set until either the shortfall has been fully mitigated or all stores are exporting as much as possible.

Many possibilities exist for establishing the discharge order. The most simple examples involve establishing a long-term fixed order, e.g. by $\overline{e}_i$, by $\overline{s}_i$, or by $\overline{h}_i$. Some dynamic alternatives, with the order changing from hour to hour are: by decreasing energy remaining, e_{it}, and by decreasing discharge times, h_{it}. As we wish if possible to avoid reducing $\min\{e_{it}, \overline{s}_i\}$ for any stores, it is clear that discharging those with the highest h_{it} first is a good strategy.

4.5.3. Proportional discharge

Another approach for multiple stores is to make coordinated decisions that seek to export from each store in proportion to it's energy content, known as the 'proportional discharge' method.

The approach involves attempting to set $s^*_{it} = \alpha e_{it}$ for some appropriate value $\alpha \in [0, 1]$. However, it may be the case that some, or all, stores are limited by their finite power capacity. Since this approach ensures that every store is able to contribute to mitigating shortfalls approximately until they are all empty, no individual store will run out of energy first (if this is indeed avoidable). The scaling factor α is obtained by solving

$$\sum_{i=1}^{N} \min\{\alpha e_{it},\ \overline{s}_i\} = \max\{d_t - x_t - y_t,\ 0\} \tag{28}$$

over $\alpha \in [0, 1]$. If no solution exists, i.e. if $\sum_{i=1}^{N} \min\{e_i, \overline{s}_i\} < d_t - x_t - y_t$, then $\alpha = 1$.

The need to solve such a problem appears to make this approach much more computationally expensive than the sequential-greedy alternative. However, a simple algorithm exists which directly determines s^*_{it}. The first step of the algorithm is to order the stores by decreasing h_{it}. Then we can sequentially calculate each s^*_{it}, through the following recursive equations:

$$\chi_1 = \varphi_t \tag{29}$$

$$E_i = \textstyle\sum_{j=i}^{N} e_{it} \tag{30}$$

$$\alpha_i = \min\{\chi_i / E_i,\ 1\} \tag{31}$$

$$s^*_{it} = \min\{\alpha_i e_{it},\ \overline{s}_i\} \tag{32}$$

$$\chi_{i+1} = \chi_i - s^*_{it} \tag{33}$$

This algorithm has been verified through systematic numerical experimentation, involving a wide variety of shortfall sequences, and no instances were found where it did not precisely solve Eq. (28). The authors intend to develop a proof that the algorithm always solves Eq. (28).

4.5.4. No universally optimal strategy: examples

Although each of the heuristic strategies in the coordination approach presented above are clearly good, neither is universally the best for all storage configurations and shortfall events. This is demonstrated in the following illustrative examples, where one method performs better than the other.

Example 1: consider a set of 2 stores at time t with power export capacities $\overline{s}_1 = 2,\ \overline{s}_2 = 2$. Their energy contents at time t are $e_{1t} = 3,\ e_{2t} = 2$, so that $\overline{s}_t^{\text{eff}} = 4$. There is a shortfall lasting 2 time-steps, with $\varphi_t = 1,\ \varphi_{t+1} = 4$. The total energy shortfall therefore exactly matches that contained in the stores, and both shortfalls can be fully mitigated so long as $\overline{s}_{t+1}^{\text{eff}} = 4$, i.e. if φ_t is mitigated without reducing the stores' effective capacity.

If the stores were coordinated according to the proportional discharge approach, the exports at time t would be $s_{1t}^* = 0.6,\ s_{2t}^* = 0.4$. Since $h_{2t} = 1$, this approach means that $\overline{s}_{t+1}^{\text{eff}} = 3.6$ and there would be an ENS of 0.4 from step $t+1$. However, if coordinated according to the sequential-greedy method, ordered dynamically with decreasing h_{it}, the exports would be $s_{1t}^* = 1,\ s_{2t}^* = 0$. In this case there is no reduction in effective capacity and therefore no unserved energy. So, in this example, the sequential method is superior.

Example 2: consider the case where the same stores have energy content $e_{1t} = 3,\ e_{2t} = 3$, and there is a shortfall lasting 2 time-steps, with $\varphi_t = 2,\ \varphi_{t+1} = 4$. So, again the total shortfall energy exactly matches the stores' content, and the shortfalls may be entirely mitigated, as long as $\overline{s}_{t+1}^{\text{eff}} = 4$.

If the stores were coordinated according to the proportional discharge approach, the exports would be $s_{1t}^* = 1,\ s_{2t}^* = 1$, and since h_{2t} is now 2, this does not decrease the effective capacity and there is no unserved energy. However, if coordinated according to the sequential-greedy method, the exports would be $s_{1t}^* = 2,\ s_{2t}^* = 0$ (where the ordering at time t is arbitrary, since the h_{it} values are equal), resulting in $\overline{s}_{t+1}^{\text{eff}} = 3$ and an ENS of 1. So, in this example, the proportional method is superior.

To summarise, in Example 1 the sequential strategy provided an advantage by 'getting rid' of additional energy capacity from store 1, while preserving the effective capacity. Where both stores had equal h_{it} values in Example 2, the equitable discharging of the proportional method was superior. However, the relative performance of the 2 approaches arose from very specific combinations of the stores' energy contents, power capacities and the shortfall at time t.

5. Case Study Application: Data

5.1. Gone Green Scenario

The data used for this paper's exemplar are based on National Grid's Gone Green (GG) Scenario [16], which presents a possible evolution for the GB power system. Installed generation capacities – both conventional and wind – were taken from the 2013 edition of the scenario, and were projections for the winter 2013/2014.

The basic method used to calculate EENS and ENS quantile values was sequential Monte Carlo simulation. Historic demand series, from the winters 2005-06 to 2011-12, were used directly – albeit rescaled to match levels in the 2013-14 GG scenario. Coincident historical wind speed series were used as an input in constructing a time series model of wind power. Details of these historical series are provided in section 5.2 and section 5.4, respectively.

Individual generating unit capacities were slightly adjusted from the original GG scenario, and thus the scenario is referred to as Adjusted Gone Green (AGG). These modifications were necessary due to the politically sensitive nature of adequacy assessment results using the original scenario. However, the results presented remain generally representative of adequacy assessment results for the GB system.

Since demand levels are considerably higher in winter, it suffices to consider this season alone, and assume that the EENS contributions from other seasons are negligible. Specifically, the 20-week period staring on the first Sunday in November is investigated, consistent with GB Capacity Adequacy Assessment studies.

5.2. Demand

The historic demand traces, upon which the EENS values are conditional, are transmission-metered values, available from [17]. Traces were obtained for 7 historical seasons: the winters of 2005-06 to 2011-12. Each series was normalised by that season's nominal peak demand, and re-scaled to the level of the chosen AGG scenario. Seperate EENS values were calculated for each of these re-scaled traces, and averaged – this is described in greater detail in section 5.5.

The relevant peak demand here is the Average Cold Spell (ACS) peak, which is defined as the median out-turn peak demand level in a winter conditional on the prevailing underlying demand patterns (with the variability in out-turn peak being due primarily to weather). The value is 55,550 MW for the 2013-14 scenario studied.

An estimate of embedded generation is added to the traces so that transmission- and distribution-connected wind are treated on a common basis. A fixed 700 MW is also added to each demand trace to account for the primary reserve response, required by the SO to cover sudden losses of infeed [18]. The SO will take emergency actions such as voltage reduction or disconnections in preference to eroding this response requirement,so a shortfall is defined in this paper as failing to meet 100% of demand plus the response requirement.

5.3. Conventional Generation

The AGG scenario contains 272 conventional generation units, with a total capacity of 68,450 MW. Individual conventional generation units are modelled as being either available at their rated capacity, or completely unavailable. The availability state of generation unit g, with capacity c_g may therefore be represented by the binary random variable X_{gt}, taking the value $x_{gt} = c_g$ when the

Table 1: Generator Availabilities and Repair Times by Fuel Type

Fuel Type	**Availability Probability**	**MTTR (hours)**
Coal/Biomass	0.88	40
Gas CCGT/CHP	0.85	50
Gas OCGT	0.92	50
Oil	0.82	50
Nuclear	0.81	150
Hydro	0.84	20
Pumped Storage	0.96	20

generator is available and $x_{gt} = 0$ otherwise. The total conventional generator availability, assuming a total of g units, is then given by

$$X_t = \sum_{g=1}^{G} X_{gt}. \tag{34}$$

It is assumed that at a given time t, the X_{gt} are all statistically independent of each other. Further, each X_{gt} is a two-state, time-homogeneous Markov chain in discrete time of hourly steps. That is, $X_{g,t+1}$ only depends on X_{gt}, and in particular it is independent of $X_{g,t-1}$, $X_{g,t-2}$, and so on. The probability of transitioning from the 'on' to 'off' state is p_g, while the probability of transitioning from the 'off' to 'on' state is q_g. So, $1/p_g$ is the mean time to failure (MTTF) and $1/q_g$ is the mean time to repair (MTTR), both in hours.

The transition probabilities are assumed identical for each generator with the same fuel type. The availability probabilities for each type were taken from the original GG scenario. These were combined with MTTR values for similar units in the 1996 IEEE Reliability Test System [19], to obtain the transition probabilities. Table 1 shows the MTTRs and availability probabilities by fuel type.

This conventional plant model reflects standard practice in the power system reliability literature, and is sufficient for the aim of demonstrating the new approach to modelling storage within an exemplar representative of practical GB adequacy assessment. If the intent is to provide a realistic prediction of risk level in a real power system, it would be necessary to consider additional detail in modelling conventional plant, including the possibility of common mode events, and whether the failure and repair processes are Markovian or if Markovian whether they have constant transition rates.

5.4. Wind Generation

The transmission-connected wind generation capacity in the AGG scenario is 10,120 GW, and there are no other types of transmission-connected renewable generators. Historical wind power traces for this scenario were available for the

7 historical winter period concurrent with the demand series. The wind power traces are derived from historical wind speed traces at the wind farm locations found in the 2013 scenario, according to NASA's MERRA dataset [20]. The wind speeds were converted to wind powers using a common power curve, then scaled to reflect the capacity at each location, and finally aggregated. The power curve was statistically calibrated so that the method produced unbiased estimates of historical metered wind power values, given the true locations and capacities of wind farms during each historical winter period. This methodology was initially developed as part of the recent GB Capacity Adequacy Assessment studies, with greater detail provided in [14].

The time series model fitted to the historical wind power traces comprises of an AR(5) process, along with a random seasonal mean, followed by a logistic transform. More detail about the model-fitting process may be found in [21]. The model equations for the aggregated wind power during hour t of winter w are:

$$\text{logit}(Y(v,t)) = Y_1(w) + Y_2(w,t) \tag{35}$$

$$Y_1(v) \sim N(\mu, \sigma_1^2) \tag{36}$$

$$Y_2(v,\cdot)|u \sim \text{AR}(\alpha_1(v), \ldots, \alpha_5(w), \sigma_2(w)) \tag{37}$$

where $Y_1(w)$ captures a yearly effect, and $Y_2(w,t)$ is an AR(5) process with zero mean. The logit transform is defined by $\text{logit}(y) = \log(t(y)/(1-t(y)))$ where $t(y) = (y-a)/(b-a)$, and in this case $a = 120$ and $b = 8900$. The choice of a, b was made on the basis of achieving the best possible approximation to a normal distribution, after the logit transform is applied. The optimal parameters mean that load factors of 0 and 1 cannot be generated in the simulation, but these values do not occur in the historical series either. The index w identifies years both in the simulation and in the training data, i.e. the historical series.

5.5. Simulation Details

For each historic demand trace, Monte Carlo simulation was used to create large samples of the balance of supply and demand, without storage. Wind traces were generated using the best-fitting AR(5) coefficients for that winter, e.g. only traces for $Y_2(w,\cdot)|(w = 2005) \sim \text{AR}(\alpha_1(2005), \ldots)$ were used in conjunction with the demand trace for the 2005/06 winter. However, unique values for the year effect $Y_1(w)$ were sampled (from $N(\mu, \sigma_1^2)$) for each simulated wind power trace. The simulations were run until either 10,000 years were obtained with non-zero ENS values, or until the number of simulated years reached a ceiling of 100,000.

Stores of different sizes were then introduced, and modelled as responding to the same samples of the supply-demand balance, according to the greedy scheme. The sample mean ENS values provided estimates of the EENS values, while ordering the sample provided estimates for ENS quantiles. Using the same samples for each investigated set of storage parameters reduced both the sampling error and the computational effort.

5.6. The Far Ahead Case

The optimisation problem to be solved for the case of far ahead decisions is that expressed in Eq. (23). The $\{X_t\}$ form a stationary process, with a distribution that may be obtained by convolution of the 2-state distribution for each conventional generator. The $\{Y_t\}$ are also a stationary process in this case, but might possess diurnal variability in other countries. Their marginal distribution was established from a sample of 70,000 wind traces (10,000 for each variant of the time series parameters). The marginal distribution of the Z_t was finally established through convolution of the Y_t and X_t distributions.

ENS values were calculated for the same 90-day demand traces used for the real-time calculations, and indeed for the same samples of generation. Solving the optimisation problem of Eqs. (23) and (24) in practice required an analytical expression for the numerically derived function $g_t(s_t)$. It was found that a 4th-order polynomial was a good fit to $\log(g_t(s_t))$, so that

$$g_t(d_t - s_t) \approx \exp\left[a_0 + a_1(d_t - s_t) + a_2(d_t - s_t)^2 + a_3(d_t - s_t)^3 + a_4(d_t - s_t)^4\right]. \tag{38}$$

One set of coefficients was fitted to $0 < d_t - s_t \leq 55000$ MWh and another for $d_t - s_t > 55000$ MWh, as accuracy in the peak demand region is particularly important.

6. Case Study Application: Results

6.1. Single Stores

6.1.1. Real-Time Decisions

Fig. 2 shows calculated EENS values for single stores making decisions in real time, after the balance of demand and available generation has realised. Investigated stores had energy capacities ranging from 0 to 10,000 MWh in increments of 200 MWh. Values were calculated for full discharge times of $\overline{h} = 1, \ldots, 5$ hours. This means that for a store with an energy capacity of e.g. 1000 MWh, results were calculated for we calculated for $\overline{s} = 200, \ldots, 1000$ MW.

The figure demonstrates that EENS values decrease smoothly with increasing energy capacity. For all $\overline{h}$ values the gradient is much steeper for smaller stores, with the sharpest change in gradient occurring at about 3000 MWh. This changing gradient is much less pronounced for higher $\overline{h}$ values. Larger stores are able to fully mitigate the majority of shortfall events, so there are limited occasions during which any further additional capacity provides any further advantage.

Fig. 2 also shows that EENS values are very similar for $h = 1$ and $h = 2$ hours, but each further restriction on the maximum power output has a similar, significant impact on EENS values. This is because there are two 'darkness peak' hours that dominate the daily EENS.It is clearly advantageous to be able to export all/almost all energy during the 2 peak hours, but there is little advantage in being able to export it all during just one of those hours. Results will vary between power systems, but many have a sharply defined daily peak, so that a small number of hours dominate the EENS.

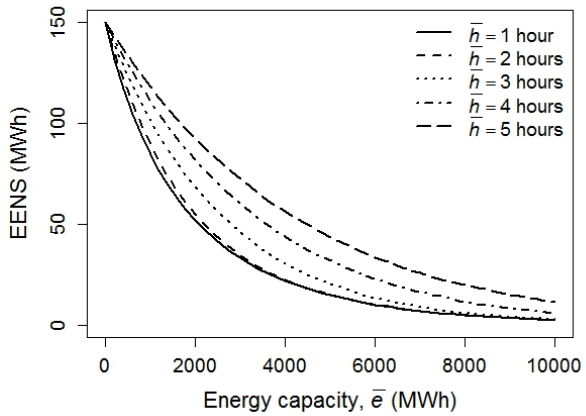

Figure 2: EENS versus energy capacity, real-time decisions, single store, various discharge times.

Fig. 3 is similar to Fig. 2, but shows the 95th percentiles of the ENS values (rather than expected values) versus energy capacity. At small storage penetrations the 95th percentile of ENS is, as expected, greater than the EENS. However at very large storage penetrations the 95th percentile of ENS is zero (i.e. the probability of there being any energy unserved in the winter is below 5%), while the EENS remains non-zero – thus above a certain storage penetration the 95th percentile of ENS is less than the EENS.

6.1.2. Far Ahead Decisions

Similar results to those presented in Fig. 2 were obtained for stores making decisions far ahead of real time, with the same set of energy and power export capacities investigated. The results are very similar to those for real-time decisions, to the extent that their plot is visually indistinguishable, and is therefore omitted. The same is true for the high quantiles of ENS.

A different type of plot is helpful to highlight subtle differences in the results. It is useful to think in terms of the reduction in EENS resulting from the presence of the stores, written as $\Delta\text{EENS}_{\text{FA}}$ and $\Delta\text{EENS}_{\text{RT}}$ for stores making far ahead and real-time decisions, respectively. From these quantities, one can define the EENS reduction ratio (EENSRR), given by $\Delta\text{EENS}_{\text{FA}}/\Delta\text{EENS}_{\text{RT}}$. The EENSRR was calculated for each investigated combination of store parameters $\overline{e}$ and $\overline{h}$, and the results are presented in Fig. 4.

It can be seen that for $\overline{h} = 4$ and $\overline{h} = 5$ hours, the EENSRR is very close to 1 for the entire $\overline{e}$ range, while the minimum value for $\overline{h} = 3$ hours is 0.99. For $\overline{h} = 2$ hours, the value of updated information is somewhat greater, with a minimum EENSRR value of 0.97. For $\overline{h} = 1$ the minimum is 0.88, for small stores. The reduction ratio concept was extended to the high quantiles of ENS,

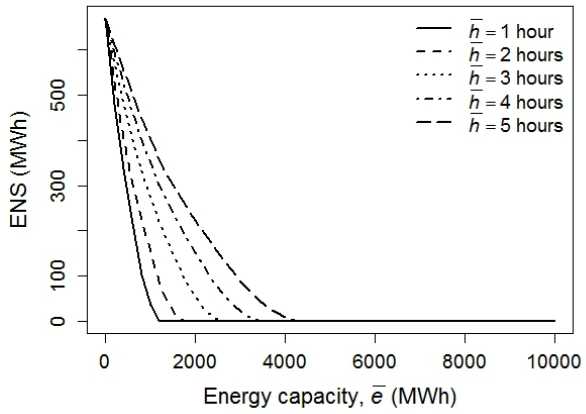

Figure 3: The 95th quantile of ENS versus energy capacity, real-time decisions, single store, various discharge times.

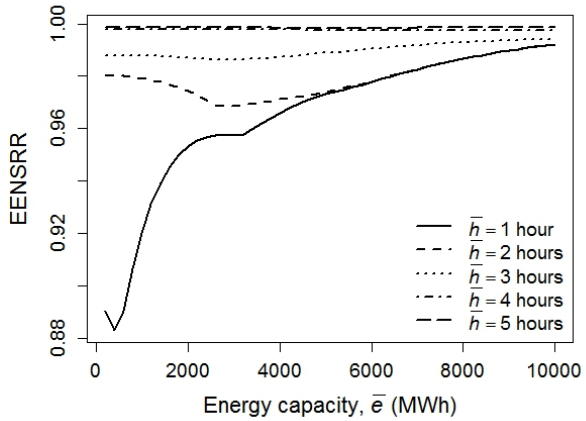

Figure 4: Ratio of EENS reductions for far ahead and real-time decisions, as a function of energy capacity, single store, various discharge times.

and the results found to be similar.

The very high overall levels of EENSRR may be attributed to the fact that the highest values of net demand ($d_t - Y_t$) occur when renewable generation is unavailable (i.e. calm days for the chosen exemplar) and demand is high. Since the demand profile is highly consistent across all days in the historical traces, shortfall events are highly predictable – almost always occurring during 3 evening hours. Strategies in the far ahead case therefore involve releasing all energy during those hours, albeit unevenly, limiting the value of real-time shortfall information. Exporting all energy during the evening is obviously not possible for $\overline{h} > 3$, but such constraints affect stores similarly for both decision-making conditions.

Some shortfall events last only 1 or 2 hours within the evening period. When such events occur, stores that can respond immediately afterwards – and are not constrained by power capacity – can release all of their energy to mitigate the shortfall. However for the far ahead case, the release of energy remains split across all high-risk hours. This is why some EENSRR values for $\overline{h} = 1$ hour are not as close to 1 as all others in the exemplar results.

The value of information would be greater than for the chosen exemplar if the daily net demand profile were broader. One factor that obviously affects this is the width of the raw demand profile – countries with a significant air conditioning load, for example, might have a broader peak. The width of the net demand peak could also be affected by strong diurnal variability in the renewable energy resource. If the renewable resource peak were well-separated form the raw demand peak, this could lead to a broadening of the net peak. However the opposite can also occur, as is the case with solar in many parts of the US, as described in [22].

6.2. Multiple Stores

This section presents results obtained for 3 scenarios involving sets of 5 stores, making decisions in real time, for a number of different coordination methods. Results were obtained for many more scenarios – involving different numbers of stores, and considerable diversity between them. It was discovered that for almost all of these scenarios, the multi-store sets were able to make almost exactly the same contribution to capacity adequacy as their single-store counterparts. The only exception is for sets where there is rather extreme variability in the relative sizes of $\overline{h}_i$ within the set, and even then, the difference vanishes towards the high end of the investigated $\overline{e}$ range. Therefore, results for only a small sample of scenarios is presented here.

The scenarios vary in 3 ways: (i) the relative sizes of the $\overline{e}_i$ within the set; (ii) the relative sizes of the $\overline{s}_i$ within the set; and (iii) the ratio of total energy and power capacities for the set. Details are presented in Table 2. Given the scenario definitions, absolute values of individual energy and power capacities may be defined by either the total energy or total power capacities for the set. The latter was chosen, labelled $\overline{e}^{tot}$, and values were matched to the values investigated for single stores.

Table 2: Details of the 3 scenarios for which results are presented. Each was scaled to match all values of energy and power capacities investigated for single stores.

Scenario	**Relative** $\overline{e}_i$	**Relative** $\overline{s}_i$	**Absolute** $\overline{h}_i$
1	[4,5,6,7,8]	[1,2,3,4,5]	[4, 2.5, 2, 1.75, 1.6]
2	[4,7,10,13,16]	[1,1,1,1,1]	[1.6, 2.8, 4, 5.2, 6.4]
3	[4,7,10,13,16]	[5,4,3,2,1]	[0.48, 1.05, 2, 3.9, 9.6]

Table 3: Ratio of EENS reduction values for multiple and single stores, various coordination methods, real-time decisions. Coordination methods: M1=Decreasing h_t, M2=Proportional Discharge, M3=Random Order, M4=Increasing h_t

Scenario	**EENSRR** $\overline{e}^{tot} = 200$ **MWh**	$\overline{e}^{tot}$ = 5000 **MWh**			
		M1	**M2**	**M3**	**M4**
1	0.99	1	1	0.99	0.99
2	0.95	0.98	0.97	0.97	0.96
3	0.71	0.92	0.92	0.91	0.89

Results were calculated for 4 methods of multi-store coordination, for each scenario. Three of these were variants on the sequential greedy discharging approach: ordering by decreasing h_{it} – close to optimal strategy; ordering randomly – i.e. no effort to coordinate beneficially; and ordering by increasing h_{it} – deliberately poor, to assess sensitivity. The final choice was the proportional discharge method. The coordination method had only a slight effect on the results. Indeed, the EENS values were identical across all methods for the smallest stores, although some difference emerge toward the middle of the investigated range (for each scenario), but the values converge toward the large capacity end of the range.

EENSRR values were again calculated, where the ratios in this case are multi-store EENS reductions divided by the corresponding single store EENS reductions. Table 3 presents a summary of these values – across scenarios and coordination methods. The table presents reduction ratios for both the smallest stores (200 MWh) and mid-range stores (5000 MWh). For the latter, separate results are presented for the various coordination methods. Only one value is presented for 200 MW stores, since the coordination method had no impact on EENSRR in this case.

The EENSRR values for scenarios 1 and 2 are consistently very high, indicating that multiple stores following a greedy strategy can contribute very nearly as much to capacity adequacy as a single store with the same total power and energy capacity – even when the method of coordination is deliberately bad. Differences in performance are more pronounced for scenario 3, reflecting

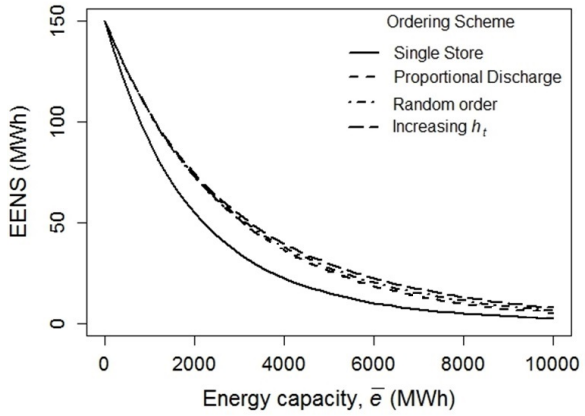

Figure 5: EENS versus $\overline{e}_{tot}$ for scenario 3 and single store with same capacities – real-time decisions, various coordination strategies. The curve for the 'decreasing h_t' method is omitted since it is indistinguishable from the 'proportional' method curve

the rather extreme $\overline{h}_i$ values within that scenario, yet most EENSRR values are again very high.

The good sequential method performed either very slightly better, or indistinguishably from the coordinated 'proportional discharge' method for each scenario. This was also true for almost all of the other scenarios investigated, but omitted here for brevity. Results for the most 'interesting' scenario, 3, are presented in Figs. 5 and 6. The former presents EENS versus $\overline{e}_{tot}$, while Fig. 6 presents EENSRR versus $\overline{e}_{tot}$. It was found that, for each scenario, the EENSRR is strictly increasing with increasing $\overline{e}^{tot}$, if slight noise is disregarded. Reduction ratio curves were also calculated for the 95th and 99th quantiles of ENS, and the results were very similar to those for EENSRR.

The extent to which multi-store and corresponding single store results differ is determined by complicated relationships involving the typical size and length of shortfalls, and the power capacity and discharge times of the stores. For example, for a power system where the most shortfall events last only one hour, then results will mostly be identical – with the exception of multiple store sets where $(\sum_{i=1}^{N} \overline{e}_i \ / \ \sum_{i=1}^{N} \overline{s}_i) \geq 1$ hour, but some stores have $\overline{h}_i < 1$ hour, and where the shortfalls are commonly of a similar size to the total power capacity of the set. If the single-period shortfalls are smaller than the total storage power capacity, then almost any conceivable set can mitigate them just as well as the corresponding single stores. If the shortfalls are typically much bigger than the power capacity, then there will be fixed difference in the stores' abilities to mitigate the shortfalls, and this difference becomes increasingly insignificant as the shortfall size increases, when EENS results are expressed as a ratio.

If the shortfall lengths are often 2 hours, then once again differences in

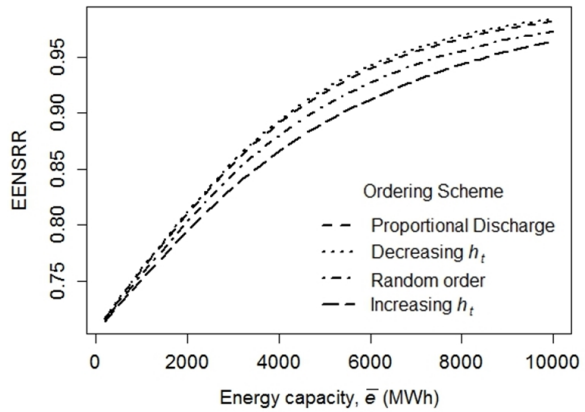

Figure 6: Ratio of EENS reductions for multiple and single stores, as a function of $\overline{e}_{tot}$, for scenario 3, real-time decisions, various coordination strategies.

performance can be significant for store sets where $(\sum_{i=1}^{N} \overline{e}_i \ / \ \sum_{i=1}^{N} \overline{s}_i) \geq 1$ hour, but some $\overline{h}_i < 1$ hour. In this case, even if the shortfall during the first time step is small compared to the total storage power capacity, the group's performance will generally be worse than the corresponding single store. For such shortfall patterns, then some differences in performance will emerge for store sets where $(\sum_{i=1}^{N} \overline{e}_i \ / \ \sum_{i=1}^{N} \overline{s}_i) \geq 2$ hours, but some $\overline{h}_i < 2$, so long as *both* shortfalls are both roughly the same size as the total storage power capacity. Generally: as the distribution of shortfall lengths shifts towards longer events, a greater variety of store sets will under-perform compared to their corresponding single stores.

6.3. Computation Times

This section presents computation times for the main calculation stages involved in producing the results, using a PC with a 2.50 GHz Intel Core i5-6500T processor and 16 GB memory. The stages were:

- *Fitting the time series model for wind and generating synthetic traces in* R: 56 seconds. The majority of the computational expense here was in simulating the season-long wind power traces, with a total of 70,000 season-long traces taking about 49 seconds (about 0.0007 s per trace).

- *Constructing shortfall sequences through Monte Carlo Simulation in* C^{++}: 30 minutes. The task here was to take the demand and wind power traces, and combine these with simulated traces of available conventional capacity to produce season-long traces of $\max(d_t - X_t - Y_t, 0)$. 1,520,220 traces were generated in order to obtain 10,000 simulated seasons with at least

one shortfall event for each historical demand trace (about 0.001 s per trace).

- *Calculating EENS values for single stores responding in real time, using* R: 2 hours 45 minutes. There were 250 storage parameter pair combinations (5 $\overline{h}$ values and 50 $\overline{e}$ values), and 7 historical seasons with 10,000 season-long traces each, making a total of 17.5 million calculations (about 0.0006 s per case).

- *Calculating EENS values for multiple stores responding in real time, using* R: 9 hours 20 minutes. Again there are 17.5 million combinations of storage parameters and margin traces, but separate EENS calculations for each coordination algorithm, all involving more complex algorithms than for a single store. For a single time step with a shortfall, calculating the response from multiple stores with the 'sequential greedy' algorithm took between 1 and 5 times longer than for a single store, with an average of about 1.5. The 'proportional discharge' approach took an average of about 3.5 times longer than for a single store (reflecting the equal number of storage scenarios with 2 and 5 stores). The total run time increased by on average slightly under half these factors, as there are other steps in the computation beyond the storage dispatch.

- *Constructing probability distributions for the total generation for each historical season, in* R: 18 minutes. The same conventional plant distribution is used for all cases, so this need only be generated once, taking about 1 minute. The marginal probability distributions associated with each of the 7 sets of wind model parameters must be generated, taking about 1.5 minutes each, and convolved with the distribution of available conventional plant, taking just under 1 minute each. Finally, each of these distributions was approximated with a polynomial function, taking about 3 seconds for all cases.

- *Solving the far ahead problem optimisation problem, using the optimization modelling language* AIMMS: 11 hours. Here the optimisation problem of Eqs. (23) and (24) must be solved for the same 90-day demand traces as used in the real time case, using the analytical approximation of Eq. (38). Separate solutions were required for each of the 7 historical seasons, and for each of the 250 storage parameter combinations – thus the average time per demand trace is about 20 s.

The language R was used for some calculation steps as built in statistical functions greatly reduce development time – it is likely that computation time could be reduced significantly by using a compiled language such as C++ (as used for simulating conventional plant traces). Thus, taking into account the software environment, the most intensive computational task in the real time case (where time series modelling is needed) is the generation of conventional plant traces.

7. Conclusions

This paper has presented a methodology for assessing the potential contribution of storage in supporting the capacity adequacy of a power system, based on a clearly stated probability model and operational strategy for the store. Results were presented for a specific exemplar based on the GB system, for stores with energy capacities ranging from 200-10000 MWh. Issues explored include the optimal strategy for a single store in mitigating energy not supplied, comparison between benefits of single and multiple stores, and the benefits of being able to wait until real time to dispatch storage instead of using a single generic storage discharge plan for all days.

The primary contribution of the paper is the methodology developed, which clearly extends to other systems where the underpinning assumptions are relevant. Caution is clearly required in extrapolating observations of modelling results obtained using the GB exemplar to other systems, however it is possible to comment on the extent to which these phenomena are likely to be GB-specific.

The similarity between risk levels when storage can be controlled in real time, and when a single generic storage schedule is used for all days, is clearly a consequence of how in GB high net demand (i.e. demand minus VG) occurs on days of high demand and low wind – and thus high net demand peaks are always similar in shape and timing to the demand peak. Thus this same observation might be made in some other systems, but not (for instance) in a system where depending on the interplay between demand and VG high net demand peaks could occur at different times.

In contrast, the similarity in performance between different algorithms for scheduling multiple stores in real time may well be repeated in most systems, as long as the depth of shortfall within a single event evolves reasonably smoothly over time. The authors hope in future work to look at data from other systems in detail, particularly for examples (such as summer peaking systems with solar generation) where the shape of the daily net demand curve is very different from that of raw demand.

Acknowledgement

G. Edwards, C.J. Dent and M.C.M. Troffaes were funded for this work by EPSRC grant EP/K002252/1 ('Energy Storage for Low Carbon Grids'). S. Sheehy was funded by an EPSRC PhD studentship.

Appendix A. Proof of Optimality of Real-Time Greedy Strategy

We wish to solve the following optimisation problem:

$$\min_s \mathbb{E}(A(s)) \tag{A.1}$$

where

$$A(s) := \sum_{t=0}^{T} b(R_t, s_t(R_t)) \tag{A.2}$$

$$b(R_t, \sigma) := \max\{0, \varphi(R_t) - \sigma\} \tag{A.3}$$

subject to the constraints

$$0 \leq s_t(r_t) \leq \overline{s} \tag{A.4}$$

and

$$\sum_{t=0}^{T} s_t(r_t) \leq \overline{e} \tag{A.5}$$

For the proof, the $\varphi_t(R_t)$ can be any functions, and the R_t can be any random variables, as long as they form a filtration, i.e. as long as R_t implies knowledge of $R_0, \ldots, R_{t-1}$. In our example, we have

$$\varphi_t(R_t) := \max\{0, d_t - X_t - Y_t\} \tag{A.6}$$

$$R_t := (X_0, Y_0, \ldots, X_t, Y_t) \tag{A.7}$$

but we don't rely on this in the proof.

Theorem 1 *The strategy s^* defined by*

$$s_t^*(r_t) := \min\{\varphi_t(r_t), \overline{s}, e_t^*\} \tag{A.8}$$

where

$$e_t^* := \overline{e} - \sum_{\tau=0}^{t-1} s_\tau^*(r_\tau) \tag{A.9}$$

minimises $A(s)$ under all possible realisations of R_T. In other words, s^* is feasible and

$$A(s^*)(r_T) \leq A(s)(r_T) \tag{A.10}$$

for all r_T and all feasible strategies s.

Before we move on to the proof, we first simplify the problem slightly.

Lemma 1 *For every feasible strategy s there is a feasible strategy s' such that $A(s) = A(s')$ and $s' \leq \varphi$.*

PROOF Let $s'_t(r_t) := \min\{\varphi_t(r_t), s_t(r_t)\}$. Clearly $s' \leq \varphi$. We are left to show that s' is feasible, and that $A(s) = A(s')$.

Clearly, it holds that $0 \leq s' \leq \overline{s}$ because both φ and s are non-negative and $s \leq \overline{s}$. Also,

$$\sum_{t=0}^{T} s'_t(r_t) \leq \sum_{t=0}^{T} s_t(r_t) \leq \overline{e} \tag{A.11}$$

because $s' \leq s$. Finally,

$$b(r_t, s_t(r_t)) = \max\{0, \varphi_t(r_t) - s_t(r_t)\} \tag{A.12}$$
$$= \varphi_t(r_t) + \max\{-\varphi_t(r_t), -s_t(r_t)\} \tag{A.13}$$
$$= \varphi_t(r_t) - \min\{\varphi_t(r_t), s_t(r_t)\} \tag{A.14}$$
$$= \varphi_t(r_t) - s'_t(r_t) \tag{A.15}$$

and because this expression is non-negative,

$$= \max\{0, \varphi_t(r_t) - s'_t(r_t)\} = b(r_t, s'_t(r_t)) \tag{A.16}$$

so it follows that $A(s) = A(s')$.

The above lemma shows that, without loss of generality, for the purpose of finding an optimal feasible strategy s, we may impose that $s \leq \phi$, and in that case the objective function becomes linear:

$$A(s)(r_T) = \sum_{t=0}^{T} \varphi_t(r_t) - s_t(r_t) \tag{A.17}$$

We are now ready identify an analytical solution.

Proof We now show that (i) s^* is feasible, and that (ii) $A(s^*) \leq A(s)$ for all feasible strategies s.

(i). By construction, $0 \leq s^* \leq \overline{s}$ so the feasibility constraint in Eq. (A.4) is satisfied. Next, if we substitute the definition of e^*_T (Eq. (A.9)) into the definition of s^*_T (Eq. (A.8)), then we immediately see that

$$s^*_T(r_T) \leq \overline{e} - \sum_{t=0}^{T-1} s^*_t(r_t), \tag{A.18}$$

from which it follows that

$$\sum_{t=0}^{T} s^*_t(r_t) \leq \overline{e} \tag{A.19}$$

and so the feasibility constraint in Eq. (A.5) is satisfied as well. So s^* is feasible.

(ii). By lemma 1, we only need to show that $A(s^*) \leq A(s)$ for feasible strategies s that satisfy $s \leq \varphi$. For such feasible strategies s,

$$A(s)(r_t) - A(s^*)(r_T) = \left(\sum_{t=0}^{T} \varphi_t(r_t) - s_t(r_t)\right) - \left(\sum_{t=0}^{T} \varphi_t(r_t) - s^*_t(r_t)\right) \tag{A.20}$$
$$= \sum_{t=0}^{T} s^*_t(r_t) - s_t(r_t) \geq 0 \tag{A.21}$$

provided that we can show that $\sum_{t=0}^{T} s^*_t(r_t) \geq \sum_{t=0}^{T} s_t(r_t)$:

a. Suppose $\min\{\varphi_t(r_t), \overline{s}\} \leq e_t^*$ for all t. Then

$$\sum_{t=0}^{T} s_t^*(r_t) = \sum_{t=0}^{T} \min\{\varphi_t(r_t), \overline{s}, e_t^*\} = \sum_{t=0}^{T} \min\{\varphi_t(r_t), \overline{s}\} \tag{A.22}$$

and now because $s \leq \varphi$ and $s \leq \overline{s}$,

$$\sum_{t=0}^{T} s_t^*(r_t) \geq \sum_{t=0}^{T} s_t(r_t) \tag{A.23}$$

b. Now suppose that there is a time τ such that

$$\min\{\varphi_\tau(r_\tau), \overline{s}\} > e_\tau^* \tag{A.24}$$

In this case,

$$s_\tau^*(r_\tau) = \min\{\varphi_\tau(r_\tau), \overline{s}, e_\tau^*\} = e_\tau^* = \overline{e} - \sum_{t=0}^{\tau-1} s_t^*(r_t) \tag{A.25}$$

and therefore

$$\sum_{t=0}^{\tau} s_t^*(r_t) = \overline{e} \tag{A.26}$$

But because s^* is feasible, we know that $\sum_{t=0}^{T} s_t^*(r_t) \leq \overline{e}$ and also that $s^* \geq 0$. Combined with the above equality, it can only be that

$$\sum_{t=0}^{T} s_t^*(r_t) = \overline{e} \tag{A.27}$$

and now using the feasibility of s,

$$\sum_{t=0}^{T} s_t^*(r_t) \geq \sum_{t=0}^{T} s_t(r_t) \tag{A.28}$$

References

References

[1] G. Strbac *et al.*, "Strategic assessment of the role and value of energy storage systems in the UK low carbon energy future," Energy Futures Lab, Imperial College London for The Carbon Trust, Tech. Rep., 2012. [Online]. Available: https://www.carbontrust.com/media/129310/energy-storage-systems-role-value-strategic-assessment.pdf

[2] ——, "Understanding the balancing challenge," Imperial College London and NERA Economic Consulting for the Department of Energy and Climate Change, Tech. Rep., 2012. [Online]. Available: http://www.nera.com/publications/archive/2012/understanding-the-balancing-challenge.html

[3] "Electrical energy storage white paper," International Electrochemical Commission, Geneva Switzerland, Tech. Rep., 2011. [Online]. Available: http://www.iec.ch/whitepaper/pdf/iecWP-energystorage-LR-en.pdf

[4] "E-storage: Shifting from cost to value 2016," World Energy Council, London, UK, Tech. Rep., 2016. [Online]. Available: https://www.worldenergy.org/wp-content/uploads/2016/03/Resources-E-storage-report-2016.02.04.pdf

[5] P. Hu, R. Karki, and R. Billinton, "Reliability evaluation of generating systems containing wind power and energy storage," *Generation, Transmission & Distribution, IET*, vol. 3, no. 8, pp. 783–791, 2009.

[6] R. Zheng and J. Zhong, "Generation adequacy assessment for power systems with wind turbine and energy storage," in *IEEE Innovative Smart Grid Technologies (ISGT), Gaithersburg, USA*, 2010.

[7] H. Wang and X. Bai, "Adequacy assessment of generating systems incorporating wind, PV and energy storage," in *IEEE Innovative Smart Grid Technologies-Asia (ISGT Asia), Tianjin, China*, 2012.

[8] A. Tuohy and M. O'Malley, "Impact of pumped storage on power systems with increasing wind penetration," in *IEEE Power & Energy Society General Meeting, Calgary, Canada*, 2009.

[9] R. Sioshansi, S. H. Madaeni, and P. Denholm, "A dynamic programming approach to estimate the capacity value of energy storage," *Power Systems, IEEE Transactions on*, vol. 29, no. 1, pp. 395–403, 2014.

[10] J. Cruise and S. Zachary, "The optimal control of storage for arbitrage and buffering, with energy applications," *preprint arXiv:1509.05788*, 2015. [Online]. Available: https://arxiv.org/pdf/1509.05788.pdf

[11] T. Gafurov, "Adequacy of generation system with large-scale deployment of solar power and energy storage," Ph.D. dissertation, Universidad Carlos III de Madrid, April 2015.

[12] S. H. Madaeni, R. Sioshansi, and P. Denholm, "Estimating the capacity value of concentrating solar power plants: A case study of the southwestern United States," *Power Systems, IEEE Transactions on*, vol. 27, no. 2, pp. 1116–1124, 2012.

[13] J. Cochran *et al.*, "Flexibility in 21st century power systems," National Renewable Energy Laboratory (NREL), Golden, CO., Tech. Rep., 2014.

[14] (2013) National Grid EMR electricity capacity report. [Online]. Available: https://www.ofgem.gov.uk/ofgem-publications/75232/electricity-capacity-assessment-report-2013-pdf

[15] Y. Zhou, P. Mancarella, and J. Mutale, "Modelling and assessment of the contribution of demand response and electrical energy storage to adequacy of supply," *Sustainable Energy, Grids and Networks*, vol. 3, pp. 12–23, 2015.

[16] (2013) National Grid electricity 10 year statement. [Online]. Available: http://www2.nationalgrid.com/UK/Industry-information/Future-of-Energy/Electricity-ten-year-statement/ETYS-Archive/

[17] National Grid: Demand data. [Online]. Available: http://www2.nationalgrid.com/uk/Industry-information/electricity-transmission-operational-data/

[18] C. Dent and S. Zachary, "Further results on the probability theory of capacity value of additional generation," in *Probabilistic Methods Applied to Power Systems (PMAPS), 2014 International Conference on*. IEEE, 2014.

[19] P. Wong *et al.*, "The IEEE reliability test system-1996. a report prepared by the reliability test system task force of the application of probability methods subcommittee," *Power Systems, IEEE Transactions on*, vol. 14, no. 3, pp. 1010–1020, 1999.

[20] M. M. Rienecker *et al.*, "MERRA: NASA's modern-era retrospective analysis for research and applications," *Journal of Climate*, vol. 24, no. 14, pp. 3624–3648, 2011. [Online]. Available: http://dx.doi.org/10.1175/JCLI-D-11-00015.1

[21] M. Troffaes, E. Williams, and C. Dent, "Data analysis and robust modelling of the impact of renewable generation on long term security of supply and demand," in *IEEE Power & Energy Society General Meeting, Denver, USA*, 2015.

[22] P. Denholm, V. Diakov, and R. Margolis, "Relative economic merits of storage and combustion turbines for meeting peak capacity requirements under increased penetration of solar photovoltaics," National Renewable Energy Laboratory, Tech. Rep., 2015. [Online]. Available: http://www.nrel.gov/docs/fy15osti/64841.pdf